Article

Why Is the Partial Molar Volume of CO$_2$ So Small When Dissolved in a Room Temperature Ionic Liquid? Structure and Dynamics of CO$_2$ Dissolved in [Bmim] [PF$_6$]

Xuhui Huang, Claudio J. Margulis, Yuhui Li, and Bruce J. Berne

J. Am. Chem. Soc., **2005**, 127 (50), 17842-17851• DOI: 10.1021/ja055315z • Publication Date (Web): 23 November 2005

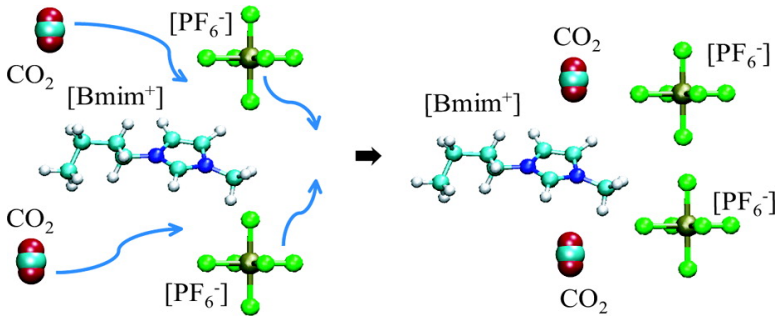

More About This Article

Additional resources and features associated with this article are available within the HTML version:

- Supporting Information
- Links to the 22 articles that cite this article, as of the time of this article download
- Access to high resolution figures
- Links to articles and content related to this article
- Copyright permission to reproduce figures and/or text from this article

View the Full Text HTML

J|A|C|S
ARTICLES
Published on Web 11/23/2005

Why Is the Partial Molar Volume of CO_2 So Small When Dissolved in a Room Temperature Ionic Liquid? Structure and Dynamics of CO_2 Dissolved in [$Bmim^+$] [PF_6^-]

Xuhui Huang,[†] Claudio J. Margulis,[‡] Yuhui Li,[†] and Bruce J. Berne*,[†]

Contribution from the Department of Chemistry and Center for Bimolecular Simulation, Columbia University, New York, New York 10027, and Department of Chemistry, University of Iowa, Iowa City, Iowa 52242

Received August 4, 2005; E-mail: berne@chem.columbia.edu

Abstract: When supercritical CO_2 is dissolved in an ionic liquid, its partial molar volume is much smaller than that observed in most other solvents. In this article we explore in atomistic detail and explain in an intuitive way the peculiar volumetric behavior experimentally observed when supercritical CO_2 is dissolved in 1-butyl-3-methylimidazolium hexafluorophosphate ([$Bmim^+$] [PF_6^-]). We also provide physical insight into the structure and dynamics occurring across the boundary of the CO_2 ionic liquid interface. We find that the liquid structure of [$Bmim^+$] [PF_6^-] in the presence of CO_2 is nearly identical to that in the neat ionic liquid (IL) even at fairly large mole fractions of CO_2. Our simulations indicate, in agreement with experiments, that partial miscibilities of one fluid into the other are very unsymmetrical, CO_2 being highly soluble in the ionic liquid phase while the ionic liquid is highly insoluble in the CO_2 phase. We interpret our results in terms of the size and shape of spontaneously forming cavities in the ionic liquid phase, and we propose that CO_2 occupies extremely well-defined locations in the IL. Even though our accurate prediction of cavity sizes in the neat IL indicates that these cavities are small compared with the van der Waals radius of a single carbon or oxygen atom, CO_2 appears to occupy a space that was for the most part a priori "empty".

1. Introduction

Room temperature ionic liquids are useful because of the wide variety of organic and inorganic molecules they are able to dissolve.[1−4] The low vapor pressure that these liquids display also makes them useful as a substitute for other more damaging organic solvents. Recently the use of CO_2 in combination with different room temperature ionic liquids has been the focus of experimental attention.[5−7] This is because of the need to generate an efficient and clean method to separate reaction products from the ionic liquid phase.[8] Supercritical CO_2 is particularly appealing as an extraction solvent because it is clean and highly soluble in the ionic liquid phase. Moreover, as Blanchard and co-workers described in their paper, interestingly the ionic liquid does not dissolve at all in the CO_2 phase.[9]

A very puzzling phenomenon occurs when one dissolves supercritical CO_2 in [$Bmim^+$] [PF_6^-] and other room temperature ionic liquids. The partial molar volume of CO_2 is much smaller in the ionic liquid (IL) phase than that in bulk supercritical CO_2 at identical temperature and pressure conditions. In fact, the partial molar volume of CO_2 is so low that CO_2 molecules dissolved in the IL phase occupy a space that is nearly equivalent to the sum of their van der Waals volume. Several very interesting papers provided experimental evidence and computational insight into the possible causes for this behavior. In particular a recent article by Maginn and co-workers[10] has ruled out the effect of acidic hydrogen attached to C2 (C2 is defined in Figure 1) as an important cause for solubility of CO_2 in the IL phase. These results are consistent with a recent article by Kazarian and co-workers[11] that through IR studies find no evidence of specific interaction of CO_2 with the imidazolium cation indicating that the role of acidic H attached to C2 is not an important factor in the solubility of CO_2. Maginn and co-workers[10] describe the strong association and particular angular orientation of CO_2 with respect to the anion. Based on the fact that radial distribution functions in the neat IL are essentially identical to those in the mixture, these authors concluded that the structure of the liquid is unchanged by dissolving CO_2. In the same article the authors propose that cations and anions form a network and CO_2 fills the interstices

[†] Columbia University.
[‡] University of Iowa.

(1) Anthony, J. L.; Anderson, J. L.; Maginn, E. J.; Brennecke, J. F. *J. Phys. Chem. B* **2005**, *109*, 6366−6374.
(2) Hanke, C. G.; Lynden-Bell, R. M. *J. Phys. Chem. B* **2003**, *107*, 10873−10878.
(3) Lynden-Bell, R. M.; Kohanoff, J.; Popolo, M. G. D. *Faraday Discuss.* **2005**, *129*, 57−67.
(4) Harper, J. B.; Lynden-Bell, R. M. *Mol. Phys.* **2004**, *102*, 85−94.
(5) Aki, S.; Mellein, B.; Saurer, E.; Brennecke, J. *J. Phys. Chem. B* **2004**, *108*, 20355−20365.
(6) Scovazzo, P.; Camper, D.; Kieft, J.; Poshusta, J.; Koval, C.; Noble, R. *Ind. Eng. Chem. Res* **2004**, *43*, 6855−6860.
(7) Camper, D.; Becker, C.; Koval, C.; Noble, R. *Ind. Eng. Chem. Res.* **2005**, *44*, 1928−1933.
(8) Fredlake, C.; Muldoon, M.; Aki, S.; Welton, T.; Brennecke, J. *Phys. Chem. Chem. Phys.* **2004**, *6*, 3280−3285.
(9) Blanchard, L. A.; Hancu, D.; Beckman, E. J.; Brennecke, J. F. *Nature* **1999**, *399*, 28−29.
(10) Cadena, C.; Anthony, J. L.; Shah, J. K.; Morrow, T. I.; Brennecke, J. F.; Maginn, E. J. *J. Am. Chem. Soc.* **2004**, *126*, 5300−5308.
(11) Kazarian, S. G.; Briscoe, B. J.; Welton, T. *ChemComm* **2000**, 2047−2048.

10.1021/ja055315z CCC: $30.25

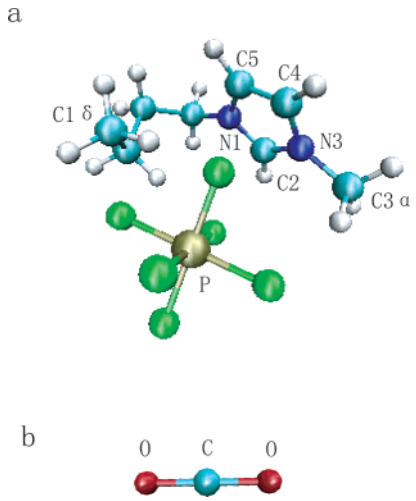

Figure 1. (a) 1-Butyl-3-methylimidazolium ([Bmim$^+$]) hexafluorophosphate ([PF_6^-]). (b) CO_2.

in the fluid. In a different paper Blanchard and co-workers[12] show how the dilation of the CO_2−ionic liquid mixture is very different from the corresponding results obtained by mixing CO_2 and 1-methylimidazole, the molecule from which the ionic solvent is synthesized. A second piece of information relevant to the issue of volume expansion is the correlation between ionic liquid molar volume and CO_2 solubility. Henry constants and other thermodynamical properties for different CO_2−IL systems have also been reported recently in several experimental and computational papers.[1,10,13−21]

2. Simulation Methods

We performed classical molecular dynamics simulations for the [Bmim$^+$] [PF_6^-]/CO_2 system schematically depicted in Figure 1. The interactions in the case of the ionic liquid were modeled by a potential function of the form

$$U = U_{\text{stretch}} + U_{\text{bend}} + U_{\text{torsion}} + U_{\text{LJ}} + U_{\text{Coulomb}} \tag{1}$$

where

$$U_{\text{stretch}} = \sum_{bonds} K_r(r - r_{\text{eq}})^2 \tag{2}$$

$$U_{\text{bend}} = \sum_{angles} K_\theta(\theta - \theta_{\text{eq}})^2 \tag{3}$$

$$U_{\text{torsion}} = \sum_{dihedrals} \sum_{i=1}^{3} V_i[1 + \cos(\phi + f_i)] \tag{4}$$

$$U_{\text{LJ}} = \sum_{i<j} 4\epsilon_{ij}[(\sigma_{ij}/r_{ij})^{12} - (\sigma_{ij}/r_{ij})^6] \tag{5}$$

$$U_{\text{Coulomb}} = \sum_{i<j} q_i q_j / r_{ij} \tag{6}$$

Stretch, bend, torsion, Lennard−Jones, and coulomb potential energy parameters were taken from the model developed by Margulis et al.[22]

For CO_2, the EPM2 model was selected based on its simplicity and accuracy in describing the supercritical region.[23,24] The EPM2 model has three collinear Lennard−Jones sites with partial charges on each atom and a fixed C═O bond length of 1.149 Å (Figure 1b). The LJ parameters for this model are $\sigma_{CC} = 2.757$ Å, $\epsilon_{CC}/k_B = 28.129$ *K*, $\sigma_{OO} = 3.033$ Å, and $\epsilon_{OO}/k_B = 80.507$ K. The coulomb parameters are $q_C = +0.6512e$ and $q_O = -0.3256e$. For Lennard−Jones interactions between unlike atoms, standard OPLS[25] geometric mean combination rules were adopted as described in eq 7.

$$\epsilon_{ij} = (\epsilon_{ii}\epsilon_{jj})^{1/2};\ \sigma_{ij} = (\sigma_{ii}\sigma_{jj})^{1/2} \tag{7}$$

In the current study, the thermodynamic state investigated is $T = 318.15$ K and $P = 200$ bar which in the case of CO_2 lies in the supercritical region.

All simulations were performed using the programs SIM and GROMACS.[26−28] GROMACS was used during the equilibration stage while SIM was used for production runs. In Gromacs, Nose−Hoover temperature coupling was used for the tempeature control[29] and Parrinello−Rahman pressure coupling was used for the pressure control.[30] In SIM, Nose Hoover chain (NHC) thermostats[31] were used for the temperature control and an Andersen−Hoover-type barostat was used for the pressure control.[32] Long-range electrostatic interactions were treated in the same way as in our previous work.[22,33] An algorithm originally proposed by Ciccotti[34] was used to propagate the equations of motion of the rigid linear CO_2 molecule. Periodic boundary conditions were applied in all directions.

The initial configuration of the IL/CO_2 binary system was prepared from the two independent bulk phases. The ionic liquid bulk phase consisted of 256 pairs of ions, and the bulk CO_2 phase initially included 1024 molecules. Both bulk phases were equilibrated by a 200 ps isothermal−isobaric (NPT) simulation. The two bulk phases were placed in contact along the *Z* direction. A number of excess CO_2 molecules were removed in order to keep the same cross section for the simulation boxes as that in the IL phase. The final production system contained 256 pairs of ions and 837 CO_2 molecules. An energy minimization of the combined system was first carried out in order to avoid steric clashes. A very long equilibration run of 21 ns in the constant pressure, temperature, and number of particles ensemble was then performed to allow CO_2 molecules to diffuse into the IL phase. Successive 500 ps NPT simulations were performed in order to generate five uncorrelated phase points taken from the last 200 ps. These configurations were used as initial conditions for five 300 ps production Microcanonical (NVE) runs. The last 200 ps of each of these NVE simulations were used to collect data.

(12) Blanchard, L. A.; Gu, Z.; Brennecke, J. *J. Phys. Chem. B* **2001**, *105*, 2437−2444.
(13) Urukova, I.; Vorholz, J.; Maurer, G. *J. Phys. Chem. B* **2005**, *109*, 12154−12159.
(14) Shiflett, M.; Yokozeki, A. *Ind. Eng. Chem. Res.* **2005**, *44*, 4453−4464.
(15) Shah, J.; Maginn, E. *J. Phys. Chem. B* **2005**, *12*, 10395−10405.
(16) Shariati, A.; Peters, C. *J. Supercrit. Fluids* **2005**, *34*, 171−176.
(17) Shariati, A.; Gutkowski, K.; Peters, C. *AIChE J.* **2005**, *51*, 1532−1540.
(18) Baltus, R.; Culbertson, B.; Dai, S.; Luo, H.; DePaoli, D. *J. Phys. Chem. B* **2004**, *108*, 721−727.
(19) Wu, W.; Zhang, J.; Han, B.; Chen, J.; Liu, Z.; Jiang, T.; He, J.; Li, W. *Chem. Commun.* **2003**, *12*, 1412−1413.
(20) Kamps, A.; Tuma, D.; Xia, J.; Maurer, G. *J. Chem. Eng. Data* **2003**, *3*, 746−749.
(21) Anthony, J.; Maginn, E.; Brennecke, J. *J. Phys. Chem. B* **2002**, *106*, 7315−7320.
(22) Margulis, C. J.; Stern, H. A.; Berne, B. J. *J. Phys. Chem. B* **2002**, *106*, 12017−12021.
(23) Harris, J.; Young, K. H. *J. Phys. Chem.* **1995**, *99*, 12021−12024.
(24) da Rocha, S. R. P.; Johnston, K. P.; Rossky, P. J. *J. Phys. Chem. B* **2002**, *106*, 13250−13261.
(25) Jorgensen, W.; Maxwell, D.; Tirado-Rives, J. *J. Am. Chem. Soc.* **1996**, *118*, 11225−11236.
(26) Stern, H.; Xu, H.; Harder, E.; Rittner, F.; Pavesse, M.; Berne, B. J. "SIM molecular dynamics simulation program", 2000.
(27) Berendsen, H. J. C.; van der Spoel, D.; van Drunen, R. *Comput. Phys. Comm.* **1995**, *91*, 43−56.
(28) Lindahl, E.; Hess, B.; van der Spoel, D. *J. Mol. Mod.* **2001**, *7*, 306−317.
(29) Hoover, W. *Phys. Rev. A* **1985**, *31*, 1695−1697.
(30) Parrinello, M.; Rahman, A. *J. Appl. Phys* **1981**, *52*, 7182−7190.
(31) Martyna, G. J.; Klein, M. L.; Tuckerman, M. E. *J. Chem. Phys.* **1992**, *97*, 2635−2643.
(32) Martyna, G. J.; Tobias, D. J.; Klein, M. L. *J. Chem. Phys.* **1994**, *101*, 4177−4189.
(33) Margulis, C. J. *Mol. Phys.* **2004**, *102*, 829−838.
(34) Ciccotti, G. *Mol. Phys.* **1982**, *47*, 1253−1264.

3. Results and Discussion

In a recent publication[9] the experimental pressure vs CO_2 mole fraction phase diagram for the mixture CO_2/[Bmim$^+$][PF_6^-] was reported. CO_2 is highly soluble in the IL rich phase at temperatures and pressures compatible with its critical point.

As is expected, by increasing the external pressure, larger mole fractions of CO_2 can be dissolved in the IL phase. A really interesting feature of this phase diagram is that there appears to be a maximum concentration of CO_2 past which increasing the external pressure does not result in a significant change in relative concentrations. At this particular CO_2 mole fraction the slope of the external pressure vs concentration in the mixture becomes almost infinite.

Moreover, experimental evidence indicates that the partial molar volume of the CO_2 dissolved in the IL phase is very small. The molar volume of bulk CO_2 at 318.15 K and 200 bar is about 55 cm^3/mol, while the partial molar volume of CO_2 in the CO_2−IL mixture is around 29 cm^3/mol. This number remains unchanged even up to mole fractions of CO_2 close to 0.5.[10] For CO_2 our simulations predict a partial molar volume of 28.4 cm^3/mol consistent with the experimentally observed value.

Our simulations and previous work by Maginn and co-workers[10,35] indicate that the structure of the IL does not significantly change after addition of CO_2; therefore several questions arise: are there large enough cavities in the liquid that are able to accommodate CO_2 molecules without perturbing the structure of the solvent and therefore without significantly increasing the total volume of the mixture? What is the physical explanation for the nearly infinite slope observed by Blanchard and co-workers?[9] Or in simpler terms, why is it impossible to "push" more CO_2 into the IL past this maximum concentration? In previous publications Margulis et al.[22] have shown that diffusive dynamics in this IL is very slow and that caging and trapping phenomena can be readily observed. Also work by Hu and Margulis[36] showed that the dynamics is glassy and heterogeneous, with different diffusive patterns for subensembles of IL molecules. It is therefore interesting to analyze the consequences that this slow IL dynamics induces on the diffusion of CO_2 as molecules cross the boundary interface between the two fluids. We will describe in later sections of this article that only small rearrangements (mostly angular) take place in the structure of the IL in order to accommodate CO_2 molecules; therefore a fair picture of the CO_2 dynamics as it enters the IL phase is that of diffusion through a fairly rigid and sticky maze. Through cage correlation functions, we show that the set of neighbors of a CO_2 molecule remains constant for fairly long periods of time supporting this view. Diffusion of CO_2 inside the IL phase is more than an order of magnitude slower than that in the bulk supercritical CO_2 phase.

3.1. Density Profiles and Distribution Functions. Figure 2a displays a typical configuration of the two fluid phases. Figure 2b and c are identical to Figure 2a except that in Figure 2b only the CO_2 is displayed and in Figure 2c only the IL is shown. It is clear from this picture that even though considerable amounts of CO_2 can be found in the IL rich phase, no IL can be found in the bulk CO_2 phase. This is consistent with all experimental observations on this system even at very high pressures. The partial miscibility of these two systems is very unsymmetrical. This is more clearly represented in Figure 3 where we see that the density of CO_2 in the bulk CO_2 phase decreases across the boundary from about 0.8 g/cm^3 to about 0.1 g/cm^3 while the density of cations and anions abruptly drops from the bulk phase value to zero in the CO_2 phase. The molar fraction of CO_2 in the ionic liquid phase is about 0.35, which is smaller than the experimental value at the same thermodynamic state. Due to the slow diffusivity that CO_2 displays in the IL phase, it may be possible that our equilibration (about

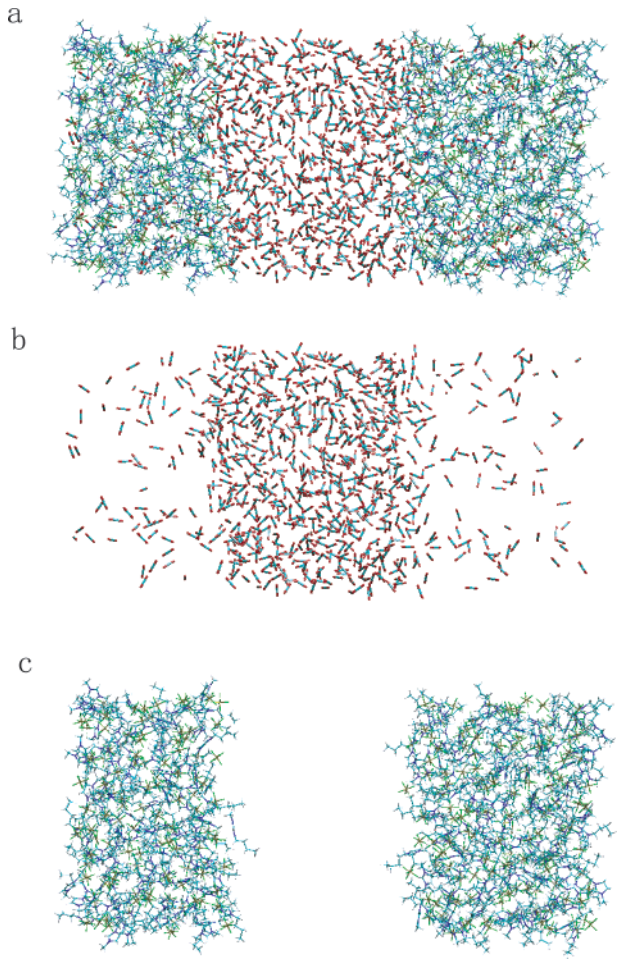

Figure 2. (a) A snapshot of the equilibrium configuration of the simulation box. (b) The same as (a) except that only CO_2 molecules are shown. (c) The same as (a) except that only the ionic liquid is shown.

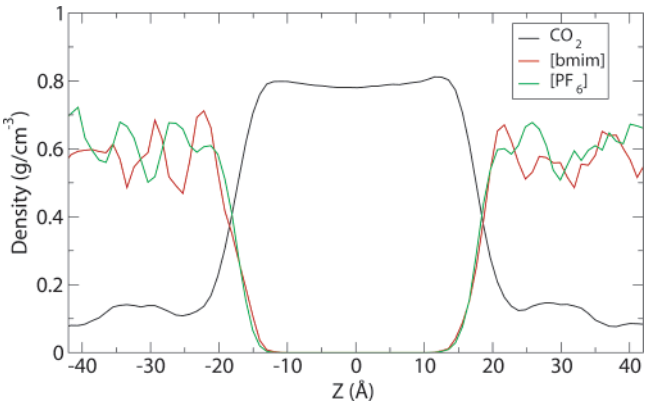

Figure 3. Average density profile for [Bmim$^+$], [PF_6^-], and CO_2 along the *z* direction.

(35) Shah, J. K.; Maginn, E. J. *Fluid Phase Equilib.* **2004**, *222*, 195−203.
(36) Hu, Z.; Margulis, C. J. Submitted to PNAS.

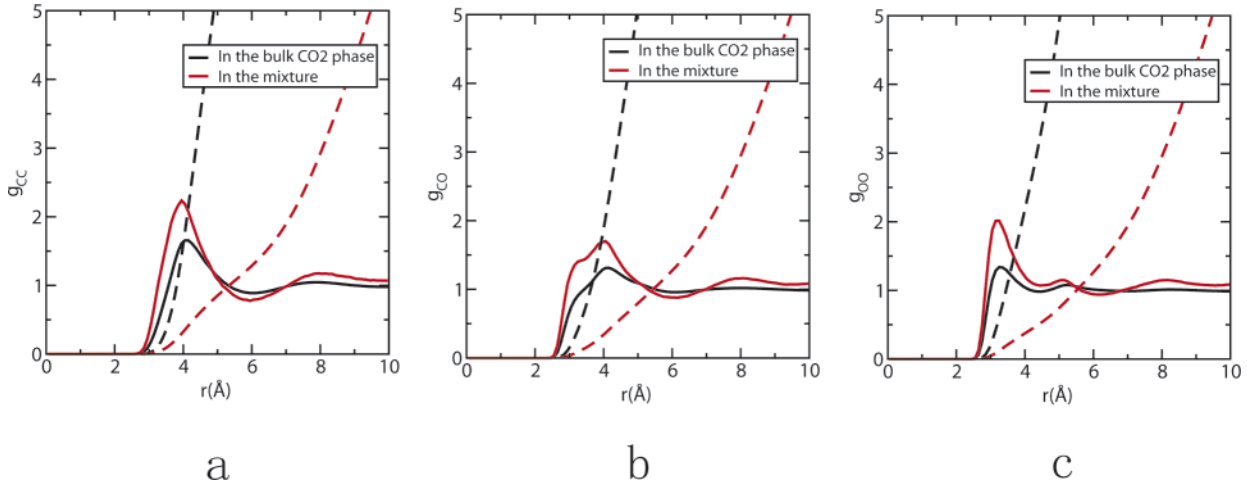

Figure 4. Comparison of the atomic RDFs (solid line) and corresponding integrals, $N(r) = \int_0^r \rho g(r) 4\pi r^2 \, dr$, in the supercritical bulk phase (black) and in the mixture phase (red). The bulk CO_2 phase is defined as a 20 Å thick layer with -10 Å $< z <$ 10 Å. The mixture phase is defined as -40 Å $< z < -30$ Å and 30 Å $< z <$ 40 Å. The RDFs in the bulk phase and in the mixture phase are normalized by the average CO_2 density in the bulk phase (about 0.8 g/cm^3) and in the mixture phase (about 0.1 g/cm^3), respectively. (a) g_{CC}, (b) g_{CO}, (c) g_{OO}.

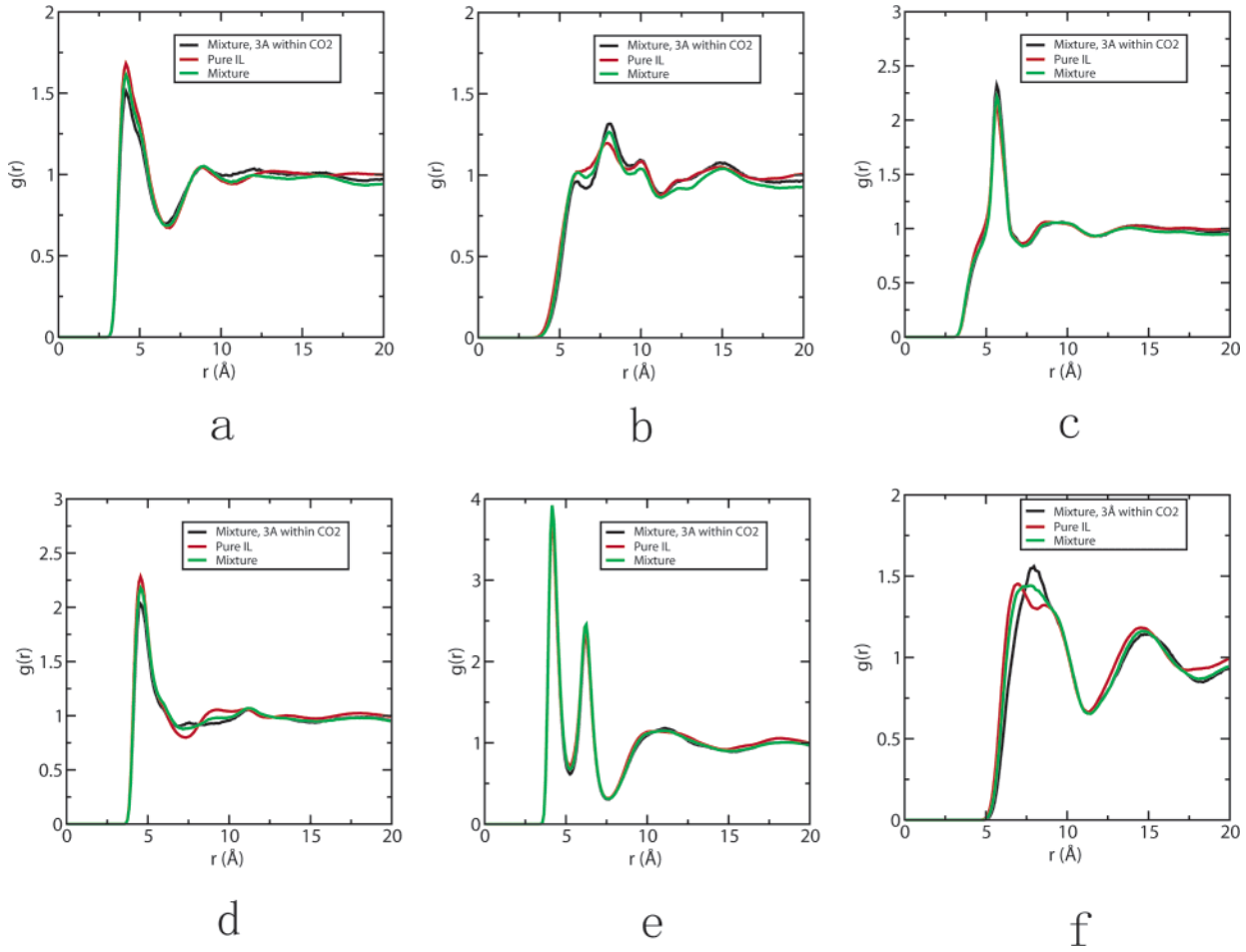

Figure 5. Comparison of atomic RDFs for the ionic liquid in the presence and absence of CO_2. The red lines are the RDFs in the pure ionic liquid. The green lines represent the RDF in the IL/CO_2 mixture. The black lines represent the RDFs in the mixture phase for only those ionic liquid molecules that are within 3 Å of a CO_2 molecule. The labels of atoms are defined in Figure 1. (a) $g_{C1\delta C1\delta}$, (b) g_{C2C2}, (c) $g_{C2C1\delta}$, (d) $g_{C1\delta P}$, (e) g_{C2P}, (f) g_{PP}.

22 ns) was not long enough to fully capture equilibrium thermodynamic conditions in the experiment. Henry's constants are in general difficult to reproduce by simulation, and small inaccuracies in the force field should be expected.

To investigate whether at the studied temperature and pressure different CO_2 molecules associate in the IL phase, we show C−C, C−O, and O−O radial distribution functions for CO_2 in the bulk CO_2 phase and in the mixture in Figure 4. It is clear that some of the structure present in the bulk CO_2 phase is still observed when CO_2 is dissolved in the IL phase; however inspection of the integral of $g(r)$ shows that in most cases a CO_2 molecule is only coordinated by 1.3 CO_2 molecules as

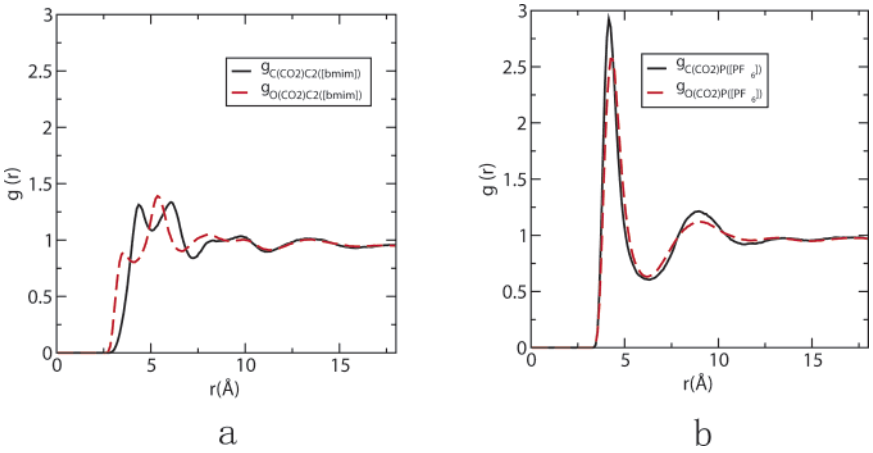

Figure 6. (a) RDF g_{CC2} between the carbon atom in CO_2 and C2 atom in [$Bmim^+$] and g_{OC2} between oxygen atoms in CO_2 and C2 in [$Bmim^+$]. (b) g_{CP} between carbon in CO_2 and P in [PF_6^-] and g_{OP} between oxygen in CO_2 and P in [PF_6^-].

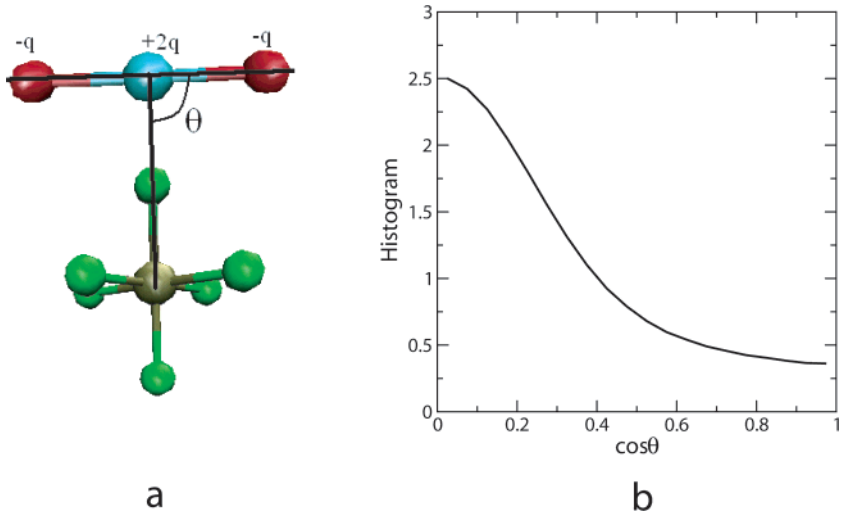

Figure 7. (a) Definition of angle between atom P and CO_2. (b) Distribution of orientations of CO_2 around atom P in [PF_6^-]. Only those CO_2 molecules in the first solvation shell of atom P are counted.

opposed to the bulk in which CO_2 is coordinated with 9.1 nearest CO_2 neighbors.

Comparing different atomic radial distribution functions for the IL in the presence and the absence of CO_2 in Figure 5 we find that these distribution functions are strikingly similar. The presence of CO_2 appears to have little to no effect on the structure of the IL even at large molar fractions of CO_2, consistent with the fact that very little swelling of this phase is observed upon dissolution of CO_2. Even more striking is the fact that the ion−ion RDFs of ions closer than 3 Å to a CO_2 molecule differ little from the ion−ion RDFs in the neat IL, except for the RDFs shown in Figure 5d and f corresponding to anion−anion and anion−alkyl chain tail of the cation.

In Figure 6, we show that CO_2 is highly associated with the anions but not with the cations. In particular it appears that CO_2 is not strongly associated with the acidic H attached to C2 (C2 is defined in Figure 1). This has been experimentally corroborated by IR measurements,[11] by substitution of this H by a methyl group, and by computer simulations.[10,37]

The results described so far indicate that if anything at all is changing, in the structure of the liquid in addition to CO_2, these changes must be small (i.e., distances between atoms in the IL are nearly the same as those in the bulk) and the most predominant changes must occur with the anions and perhaps the alkyl tails of the cation. It is important to notice however, as will be discussed in detail in subsequent subsections, that radial distribution functions may remain nearly constant while angular distributions could potentially show more significant changes. As opposed to the case of the cation in which CO_2 shows very poor association, in the case of the anion CO_2 shows strong association adopting typical "T" shape configurations that have also been observed in previous studies of CO_2 solvation with iodide.[38] The orientational distribution of CO_2 with respect to the anions is depicted in Figure 7.

The strong association between CO_2 and the anions can be ascribed to the large charge-quadrupole moment interaction between the two. As opposed to the case of [PF_6^-], in which the charge distribution is localized, in the case of [$Bmim^+$], the charge distribution is delocalized around the ring and Coulomb interactions with CO_2 are likely to be weaker.

3.2. Free Space Hypothesis and the Voronoi Cavity Distribution. Several experimental and computational articles suggest that perhaps CO_2 is taking up free space from cavities already available in the rigid and intricate topography of the ionic liquid.[6] Therefore it is important to quantify the size of

(37) Deschamps, J.; Gomes, M. F. C.; Padua, A. A. H. *ChemPhysChem* **2004**, *5*, 1049−1052.
(38) Margulis, C. J.; Coker, D. F. *J. Chem. Phys.* **1999**, *110*, 5677−5690.

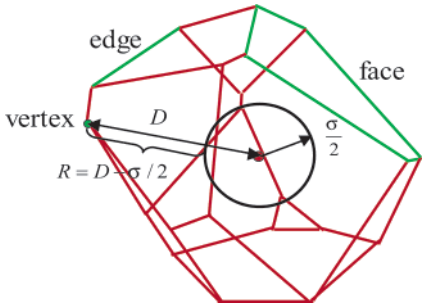

Figure 8. A typical VP in the system is shown. The red point represents the center of the particle with radius $\sigma/2$. Green point, segment, and polygon are examples of VP vertex, VP edge, and VP face, respectively. D is the distance between the specified vertex and the corresponding particle, and σ is the Lennard−Jones parameter of the particle. Therefore the radius of the spherical cavity is $R = D - \sigma/2$.

typical cavities in the liquid before CO_2 is introduced. In a recent paper Margulis[33] has roughly estimated the distribution of the size of cavities for imidazolium based ionic liquids with different alkyl chain lengths using a simple approach based on analyzing the free space around randomly distributed points in the liquid. In this work, we instead use the Voronoi algorithm,[39−41] a more mathematically rigorous way of studying the topology of the cavities inside a liquid. In the Voronoi method the whole space is divided into Voronoi polyhedra. The Voronoi polyhedra (VP) are nonoverlapping and fill all the space of the system.[42] Since the cation [$Bmim^+$] has a very anisotropic shape and different components of the ionic liquid and CO_2 molecules have quite different volumes, each atom in the IL (except for hydrogens) was described as a single spherical particle with a radius equal to its atomic van der Waals radius. (The van der Waals radius of carbon atoms to which hydrogen atoms are connected was scaled to include the size effect of the hydrogen atom.) Using the coordinates of the atoms (except for hydrogens) and the method described by Ruocco et al.,[40] we built the VP of individual atoms. All the vertices and the indices of four atoms whose VP share a certain vertex have been determined. A typical VP in the system is shown in Figure 8. Since VP vertices have equal distances to the adjacent four particles, they sit at the centers of the possible cavities in the liquid. The radius of such cavities can be easily computed by subtracting the van der Waals radius of the atom from the distance between the VP vertex and the four nearest particles (see Figure 8). In this way we obtained the largest radius of a spherical cavity which can exist at the vertex. After all the vertices were investigated, we computed the size distribution of spherical cavities in the liquid. The summation of the volume of these spheres gives a lower bound limit to the total empty volume in the liquid. Figure 9a shows the number of spherical cavities per ion pair with a given radius R, and Figure 9b shows the distribution of spherical cavities in the neat liquid and the mixture. See the footnote for a technical details of how the Voronoi polyhedra are constructed (ref 42).

Even though CO_2 is not a spherical molecule, these graphs show that pre-existing cavities in the liquid are small compared with the van der Waals size of a carbon or oxygen atom (1.5 Å), and therefore it is clear that there are no sufficiently large cavities in the solvent that can accommodate CO_2 without some sort of rearrangements in the IL phase. It is therefore puzzling that radial distribution functions for the IL do not appreciably change upon introduction of CO_2 and also that the partial molar volume of CO_2 in the mixture at a CO_2 mole fraction larger than 0.3 is extremely small. How can we explain these two findings?

3.3. Three-Dimensional Distributions. To better understand the structural changes occurring in the ionic liquid phase as CO_2 molecules are introduced in the system, we must take into account not only radial distributions but also the average relative angular orientation between different species. As mentioned before radial distribution functions in the IL appear to be fairly insensitive to the presence of CO_2 even at a relatively high molar fraction of CO_2.

A way to study such combined radial-angular distributions is by generating three-dimensional isosurfaces of the four dimensional density defined as X, Y, Z, $\rho(X, Y, Z)$. Here X, Y, Z are relative body frame coordinates. X and Y lie in the plane of the imidazolium ring with X pointing in the direction of the bond between nitrogen and the first carbon atom belonging to the longer alkyl chain. Z points perpendicular to the imidazolium ring; its direction is chosen by following the usual right-hand rule (see Figure 13a).

Using these definitions we computed the relative positions of anions with respect to the aforementioned set of the fixed body frame axis in the presence and absence of CO_2. Figure 10a and b show these distribution functions from two different angular perspectives. In both cases displayed on the left are the results for the neat liquid, and on the right, those corresponding to the mixture.

One interesting finding is that no significant anionic density is present right above or below the imidazolim ring neither in the neat liquid nor in the solution phase. The distributions are similar in both cases except that in the case of the mixture anions are angularly closer to the plane of the ring. As one can appreciate in Figure 10, the contour surfaces above and below the ring are connected in the mixture, while in the neat IL they are separated.

Using the same coordinate system we computed distribution functions of the relative position between cations and the center of mass of CO_2. We only considered those cations within 3 Å of a CO_2 molecule. The results are displayed in Figure 11. It is clear that most of the CO_2 density can be found perpendicular to the imidazolium rings, both above and below, as well as near the long alkyl chain. From the Voronoi polyhedra analysis we know that there are no sufficiently large cavities to accommodate CO_2 molecules in the neat IL. What sort of rearrangement takes place in order to accommodate CO_2?

(39) Okabe, A.; Boots, B.; Sugihara, K. *Spatial Tessellations: Concepts and applications of voronoi diagrams;* Wiley: New York, 1992.
(40) Ruocco, G.; Sampoli, M.; Vallauri, R. *J. Chem. Phys.* **1992**, *96* (8), 6167−6176.
(41) Jedlovszky, P. *J. Chem. Phys* **2000**, *113* (20), 9113−9121.
(42) The Voronoi algorithm is a method that belongs to the classical problem of computational geometry of disordered systems.[39] By definition, any point in the voronoi polyhedra (VP) of a particle is always closer to this particle than to any other particles in the system. The union of all the VPs is known as the Voronoi diagram, which is a spatial tessellation and unequally divides the space into polyhedra without any overlapping. The key to building the VP is to find the vertices, the edges, and the faces of every VP. The face separating two adjoining VP of two adjacent particles is a VP face, an assembly of points equally far from these two particles. Three neighboring VP share an edge, the points on which have the same distance to the three adjacent particles. Each vertex is identified by three VP faces and has equal distances to four particles, the VP of which share the same vertex. A typical VP is shown in Figure 8. (As has been discussed before in previous publications,[40,41] in a molecular liquid, there is only a very small probability for four VP faces to intersect at the same point.)

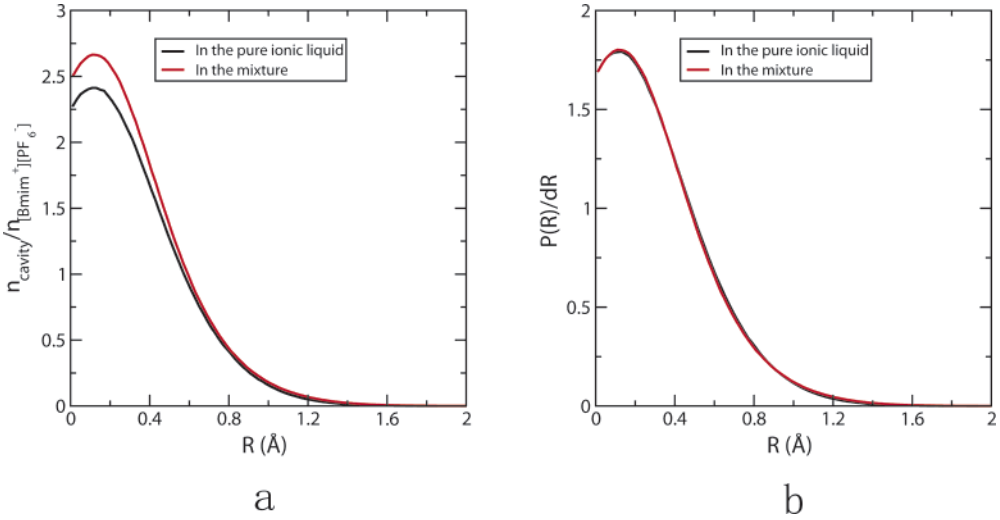

Figure 9. (a) Average number of cavities per ionic liquid molecule [$Bmim^+$][PF_6^-] with certain radius vs the radius in the pure IL (black line) and in the IL/CO_2 mixture (red line). (b) Distribution of radii of all spherical cavities in the neat IL (black line) and in the IL/CO_2 mixture (red line) generated by Voronoi analysis.

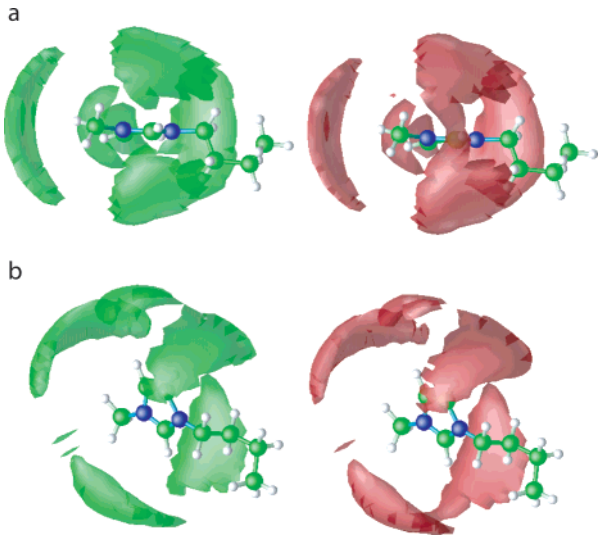

Figure 10. (a) Three-dimensional probability distribution of atom *P* in [PF_6^-] around [$Bmim^+$] in neat ionic liquid (left) and in the IL−CO_2 mixture (right). In the IL−CO_2 mixture, only those ionic liquid molecules that are within 3 Å of a CO_2 molecule are used for the computation. The contour surfaces enclose regions containing an excess of P. The cutoff value for these regions is 7 times of the average concentration of P in the liquid. (b) The same as (a) except from another perspective.

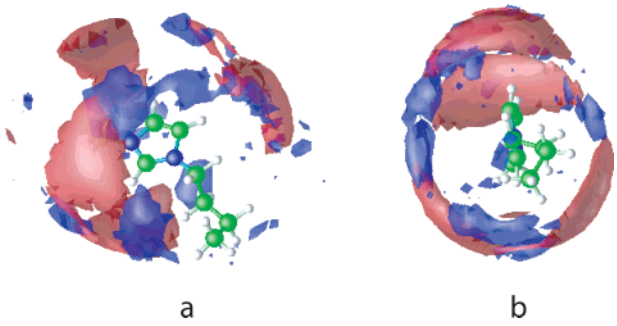

Figure 11. (a) Three-dimensional probability distribution around [$Bmim^+$] in the IL−CO_2 mixture for those ionic liquid molecules that are within 3 Å of a CO_2 molecule. The contour surfaces in red enclose regions containing an excess of P in [PF_6^-]. The cutoff value for these regions is 7 times the average concentration of P in the liquid. The contour surfaces in blue enclose regions containing an excess of C in CO_2. The cutoff value for these regions is 5 times the average concentration of C in the liquid. (b) The same as (a) except from another perspective.

Figure 12 explains pictorially how, by introducing small anionic angular displacements toward the plane of the imidazolium ring, enough space can be created above and below the ring that can accommodate CO_2 molecules. This can be appreciated in Figure 10 but is most clearly demonstrated in Figure 13. In Figure 13 we show the relative orientational distribution function $f(\theta,\phi)$ for anions that are within 6 Å of an imidazolium ring (the coordinate system is shown in the Figure 13a). Only those IL molecules within 3 Å of a CO_2 molecule are considered. Results are displayed in the case of the neat liquid and the mixture.

It is clear from Figure 13b that the angular distribution is nearly identical in the neat liquid and in solution. The addition of CO_2 molecules only causes significant changes at values of $\cos(\phi) = -1$. These changes are due to the small angular displacements described in Figure 12. It is also evident from our data that these angular displacements do not significantly affect radial distribution functions while still permitting CO_2 to fit in "empty" volume originally available in the ionic liquid. As our Voronoi calculations prove, this empty volume in the neat liquid is mostly available not as cavities of the size of a CO_2 molecule but as a collection of smaller cavities that reorganize into a smaller number of larger voids upon introduction of CO_2. This phenomenon of reorganization of "empty space" in the liquid accounts for the small change in volume as CO_2 is added to the ionic liquid phase.

One outstanding issue remains to be addressed. As can be appreciated from the phase diagram reported in a previous article,[9] there exists a maximum CO_2 concentration above which no more molecules can be dissolved even when very high pressures are imposed on the two phase system (CO_2−IL mixture/pure supercritical CO_2). The diagram of the pressure versus mole fraction displays a nearly infinite slope at a mole fraction of CO_2 of about 0.8. We conjecture that at this mole fraction most of the cavities that can be generated by small angular displacements have already been occupied and further insertion of CO_2 would require "breaking" the cohesive structure of the ionic liquid.

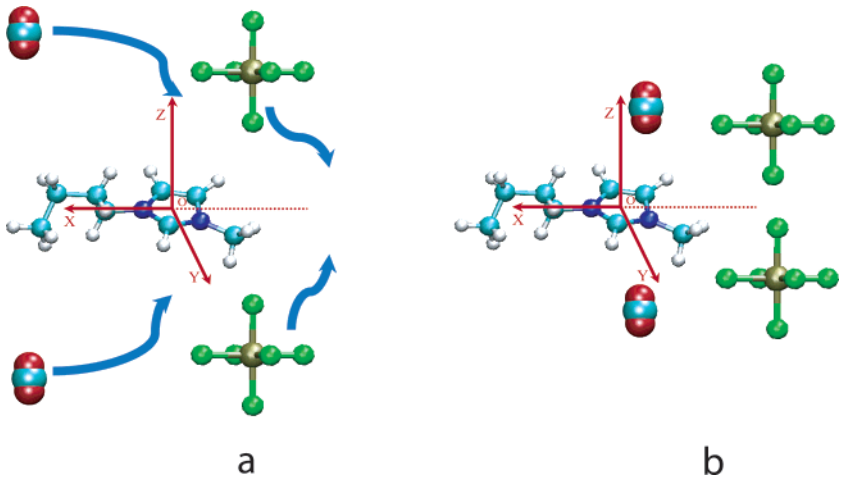

Figure 12. (a) The sketch shows the relative positions of [PF_6^-] and [$Bmim^+$] in the neat IL. The arrows approximately indicate the directions in which anions displace to accommodate CO_2 in solution and the most probable location of CO_2.

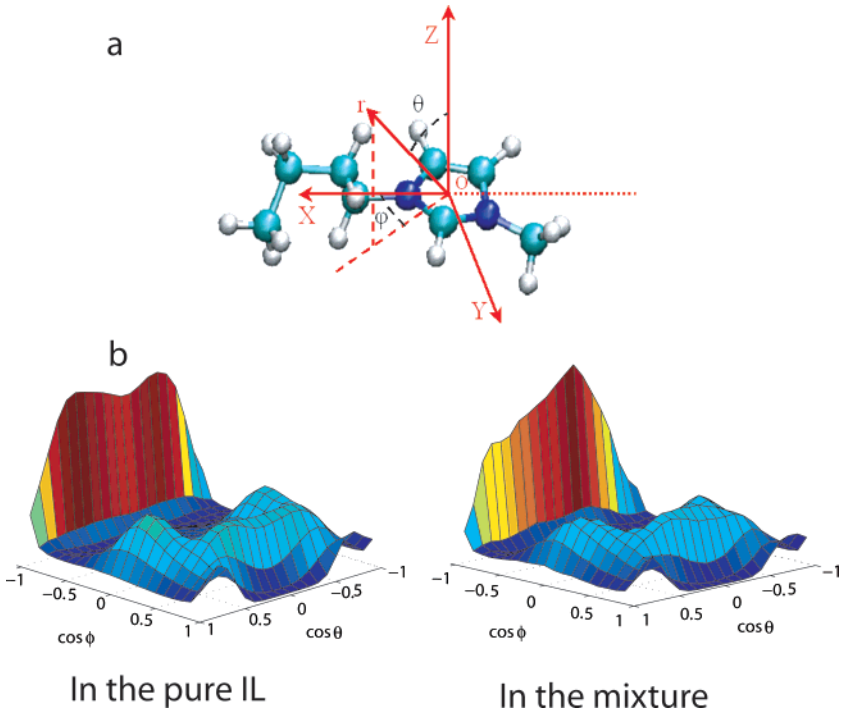

Figure 13. (a) Coordinate system. The origin is the center of mass of all the atoms on the five-member ring. Angles θ and ϕ are defined. (b) The angular distribution (cos θ, cos ϕ, P(cos θ, cos ϕ)) of atom P in [PF_6^-] in the shell 0 Å to 6 Å around [$Bmim^+$] is shown in the neat ionic liquid (the graph on the left) and in the IL−CO_2 mixture (the graph on the right). In the IL−CO_2 mixture, only those ionic liquid molecules that are within 3 Å of a CO_2 molecule are used for the computation.

3.4. Cage Correlation Functions and Diffusive Dynamics across the Interface. In previous sections we described the diffusive behavior of CO_2 in the ionic liquid phase as that of a particle percolating through a quasi rigid maze. What we mean by this is not that the IL is not fluid but that the time scale on which ions move in the mixture is much slower than the time on which CO_2 does. Table 1 shows diffusion constants for molecules and ions computed from our simulations. The diffusion constant of CO_2 in the IL is about 10 times larger than that of the ions and is about 46 times smaller than that in the bulk supercritical CO_2 phase. The slow IL diffusive dynamics observed here is consistent with previous work by Del Popolo and Voth[43] describing the non-Gaussian behavior of van-Hoove correlation functions in 1-butyl-3-methylimidazolium hexafluorophosphate and the work of Hu and Margulis[36] indicating that this and other similar ILs show the signs of heterogeneity typically found in glassy environments. Figure

Table 1. Diffusion Constants of CO_2, [$Bmim^+$], and [PF_6^-] in the Various Phases

CO_2	bulk CO_2 phase	mixture phase
D (Å^2/ps)	1.83 ± 0.05	0.040 ± 0.007
[$Bmim^+$]	neat ionic liquid	mixture phase
D (Å^2/ps)	0.008 ± 0.002	0.0077 ± 0.0009
[PF_6^-]	neat ionic liquid	mixture phase
D (Å^2/ps)	0.007 ± 0.002	0.0068 ± 0.0009

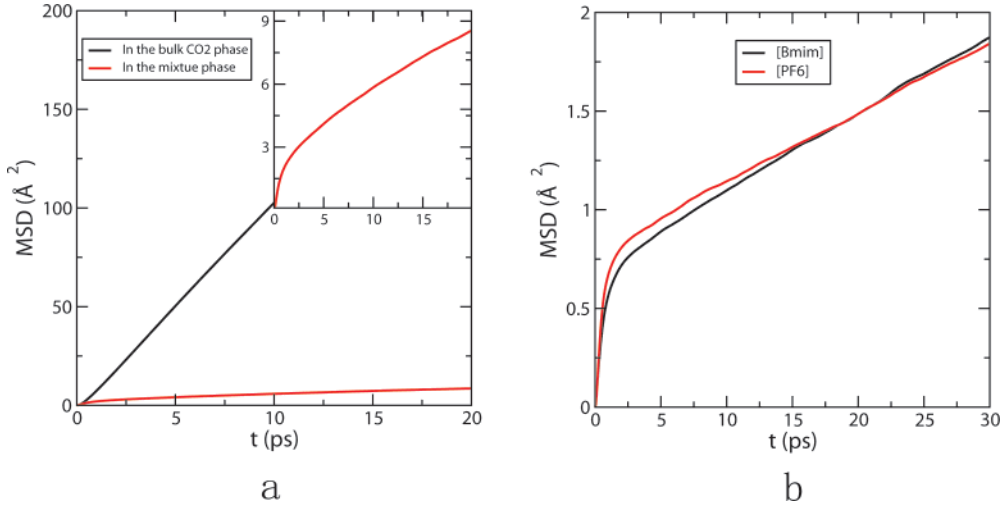

Figure 14. (a) Comparison of the mean square displacement for the center of mass of CO_2 molecules in the bulk CO_2 phase (black) and in the IL−CO_2 mixture (red). (b) Comparison of the mean square displacement for the center of mass of [$Bmim^+$] (black) and the center of mass of [PF_6^-] (red) in the IL−CO_2 solution phase.

14 displays a comparison of the mean square displacement as a function of time for the different species in each of the phases. From this we see that both the ions and CO_2 display nonballistic, nondiffusive intermediate caging regimes that last for a few picoseconds before the diffusive regime is established. During this nondiffusive regime CO_2 is able to explore a larger volume than the ions as can be appreciated by the fact that at 2.5 ps the msd for CO_2 in the IL rich phase is about 3 Å^2 while in the case of the ions the MSD is less than 1 Å^2. The diffusion constants computed here for CO_2 and [$Bmim^+$][PF_6] were obtained from 5 NVE simulation of 200 ps in duration. It is likely that the results for CO_2 are more accurate than those for the IL for which longer simulations might be required in order to fully reach the linear diffusive regime.[36]

It is instructive to analyze the diffusion constant of CO_2 as molecules cross the interface from the bulk supercritical fluid to the mixture. Figure 15 shows D_x diffusion constants in different slices of liquid along the Z direction ($\hat{Z}$ is taken as the vector perpendicular to the interface). The diffusion coefficients of different slices of liquid parallel to the interface were computed in the following way:[44]

$$D_{xx}(a, b) = \lim_{\tau \to \infty} \frac{\langle \Delta x(\tau)^2 \rangle_{a,b}}{2\tau P(\tau)} \tag{8}$$

where,

$$\langle \Delta x(t)^2 \rangle_{a,b} = \frac{1}{T} \sum_{t=1}^{T} \frac{1}{N(t)} \sum_{i \in \zeta(t,\, t+\tau)} (x_i(t+\tau) - x_i(t))^2 \tag{9}$$

and

$$P(\tau) = \frac{1}{T} \sum_{t=1}^{T} \frac{N(t, t+\tau)}{N(t)} \tag{10}$$

Here $\zeta(t, t + \tau)$ represents the set of all particles that stay in the layer $\{a, b\}$ during the time interval between t and $t + \tau$.

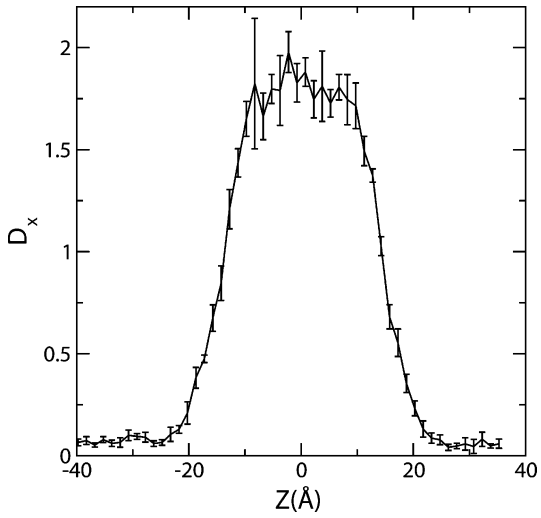

Figure 15. Plot of the diffusion coefficient D_x in different slice of liquid parallel to the interface.

$N(t, t + \tau)$ is the number of such particles. $N(t)$ is the number of particles in the layer at time t. T is the total number of time steps. $P(\tau)$ is the survival probability. Several interesting pieces of information can be extracted from these calculations. The "local" diffusion constant of CO_2 changes monotonically from the value in the bulk CO_2 phase to the value inside the IL rich phase on a length scale of about 10 Å. Notice that the change in D_x happens on a longer length scale than the actual density profile change in Figure 3. This phenomenon has been observed before[45] in water liquid−vapor simulations.

To better understand the disparity of time scales for dynamics occurring in the CO_2−IL mixture, we computed cage−cage correlation functions originally introduced by Berne and coworkers.[46] These correlation functions accurately measure the time scale on which a CO_2 molecule loses memory of the identity of its neighboring molecules.

(43) Popolo, M. G. D.; Voth, G. A. *J. Phys. Chem. B* **2004**, *108*, 1744−1752.
(44) Liu, P.; Harder, E.; Berne, B. J. *J. Phys. Chem. B* **2004**, *108*, 6595−6602.
(45) Liu, P.; Harder, E.; Berne, B. J. *J. Phys. Chem. B* **2005**, *109*, 2949−2955.
(46) Rabani, E.; Gezelter, J. D.; Berne, B. J. *J. Chem. Phys* **1997**, *107* (17), 6867−6876.

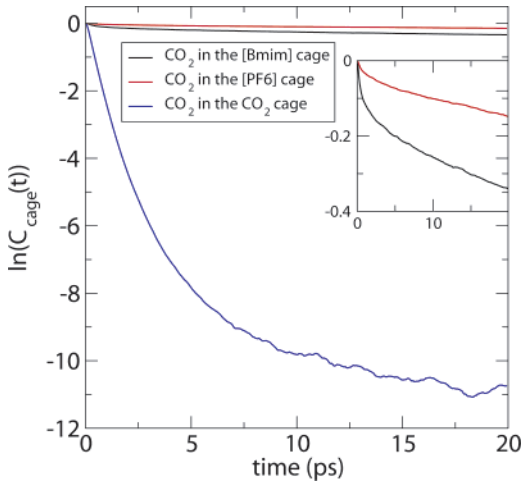

Figure 16. Cage correlation functions for CO_2 molecules in the IL rich phase and in the supercritical CO_2 phase. [$Bmim^+$] (black), [PF_6^-] (red), neat CO_2 phase (blue).

The cage correlation function is defined in the following way,

$$C_{\text{cage}}^{\text{out}}(t) = \langle \Theta(1 - n_i^{\text{out}}(0, t)) \rangle \tag{11}$$

Here the label "*i*" stands for the center of mass of CO_2 molecule "*i*", and $n_i^{\text{out}}(0, t)$ is the number of neighboring molecules that have left molecule *i*'s original neighbor list at time *t*. The quantity $n_i^{\text{out}}(0, t)$ is easily computed as

$$n_i^{\text{out}}(0, t) = | l_i(t)|^2 - l_i(0) \cdot l_i(t) \tag{12}$$

where the generalized neighbor list l_i is a vector of length *N* defined as

$$l_i \equiv \begin{pmatrix} f(r_{i1}) \\ \vdots \\ f(r_{iN}) \end{pmatrix} \tag{13}$$

and $f(r_{iN})$ is the Heaviside function.

$$f(r_{ij}) = \Theta(r_{\text{nlist}} - r_{ij}) = \begin{cases} 1 & \text{if } r_{ij} < r_{\text{nlist}} \\ 0 & \text{otherwise} \end{cases} \tag{14}$$

r_{nlist} is the neighbor list cutoff radius which in the present study was chosen as the first solvation shell in the liquid.

From these definitions it is easy to see that $|l_i(t)|^2$ is the number of atoms in *i*'s neighbor list at time *t*, while $l_i(0) \cdot l_i(t)$ is the number of molecules that are in *i*'s neighbor list both at time 0 and at time *t*.

By looking at the cage−cage correlation functions in Figure 16 we see that in the bulk CO_2 phase a CO_2 molecule loses memory of its neighbors within about 2 ps. On the other hand in the ionic liquid at time scales of 20 ps or even longer the natural logarithm of this correlation function is essentially zero indicating no loss of memory. In fact the loss of memory occurs on a much longer time scale.

4. Conclusions

When CO_2 at supercritical conditions shares an interface with [$Bmim^+$][PF_6^-], it readily dissolves in the IL phase but the IL does not dissolve at all in the CO_2 phase. In fact our studies indicate that this dissolution is characterized by a process very similar to percolation through a "quasi static" glassy material. The separation of time scales between the diffusion of CO_2 in the IL phase and that of the ions reflected both in our computed diffusion constants and cage correlation functions supports this view of CO_2 percolating through a semirigid and sticky (due to strong Coulomb attractions) glassy structure. This view is consistent with observations by Hu and Margulis[36] and by Del Popolo and Voth[43] describing the non-Gaussian characteristics of some room-temperature ILs. We also find that when we plot the diffusion constant profile for CO_2 as it crosses the interface, this function varies on a longer length scale than the changes in the density itself indicating that boundary effects extend several Å inside each of the fluid phases.

Not only is the dynamics of the IL slower than that of the CO_2 dissolved in it, but also we have recently found in preliminary studies that even when applying pressures several orders of magnitude higher no significant changes in the volume of the IL rich phase is observed even though the volume of the supercritical CO_2 significantly diminishes. The IL rich phase is highly incompressible, and its vapor pressure is negligible. We also conclude from this work and from previous experimental and computational studies that the volume of the IL does not change significantly upon dissolution of high concentrations of CO_2. We have analyzed this phenomenon in detail and find from our simulations that most of the space occupied by CO_2 in the IL phase consists of very localized cavities of larger size than those spontaneously forming in the neat IL as opposed to the previous hypothesis found in the literature. These larger cavities are for the most part not generated by expansion of the IL phase, but instead they are formed by small angular rearrangements of the anions. With these small angular rearrangements that do not significantly change radial distribution functions in the liquid, CO_2 is able to fit above and below the imidazolium ring. CO_2 is also typically found close to the long alkyl tail of the imidazolium ring. From the experimental work of Blanchard[9] and co-workers we see that there is a maximum concentration of CO_2 above which applying higher pressure on the system will not significantly increase the CO_2 mole fraction. We believe that above this maximum concentration, the liquid structure of the ions would have to significantly change in order to accommodate more CO_2.

Acknowledgment. This work was supported by a grant to B.J.B. from the National Science Foundation (CHE-03-16896) and from an SUR Grant from the IBM Corporation for an IBM LINUX CLUSTER. This grant was also supported by Grant PRF-G(#41450-G6) from the American Chemical Society and by internal Grant MSFP(#85022915) from the University of Iowa awarded to C.J.M. We thank Dr. Mario del Popolo and Prof. Ruth M. Lynden-Bell for providing us with template scripts to create 3D distribution functions using OpenDX. OpenDX is the open source software project based on IBM's visualization data explorer (http://www.opendx.org/).

JA055315Z